Progress In Electromagnetics Research B, Vol. 27, 83–99, 2011

ON SIMULATING THE RADIO SIGNAL PROPAGATION IN THE REVERBERATION CHAMBER WITH THE RAY LAUNCHING METHOD

K. Staniec and A. J. Pomianek

Institute of Telecommunications, Teleinformatics and Acoustics
Wroclaw University of Technology, Wroclaw, Poland

Abstract—The modeling of the reverberation chamber with the use of deterministic techniques, one of which is the Ray Launching (RL) method, requires a careful tuning with measurements. A few factors that most severely influence the simulation results are: the minimum number of stirrer rotations to produce representative outcomes, the number of reflections of each traced ray and, finally, the size of the receive probe and the wall reflection loss. In the course of investigations it was demonstrated that these factors have a different, and in some instances — even opposite, impact on the simulated results in the electromagnetic (EM) power domain and in the time domain (the time delay spread). A simple procedure consisting of a few steps has been proposed for tuning deterministic RL models to the measured data.

1. INTRODUCTION — DETERMINISTIC PROPAGATION MODELS

The class of deterministic (analytical) models is a relatively new invention and since some of them require the use of fast computation machines, their application had been rather limited until more or less the last decade. However, as will be demonstrated later in this chapter, encouraging results can be obtained with these models in both electromagnetic (EM) power domain and in the time domain. What makes them a particularly valuable tool for predicting the EM waves propagation is the fact, that they imitate the actual EM wavefront. Hence, all propagation phenomena such as reflection, attenuation and diffraction, can be easily accounted for. Also, the indoor environment can be described on a site-specific basis rather than a category basis (as is the case with statistical or empirical models).

Received 22 October 2010, Accepted 17 November 2010, Scheduled 28 November 2010
Corresponding author: Kamil Staniec (kamil.staniec@pwr.wroc.pl).

By and large the most commonly used deterministic model is one based on the technique named *ray tracing* (with numerous derivative techniques). It has been successfully applied to modeling radio coverage in small and microcells [1–4], although most suitably to indoor environments [5–7]. An interesting application — in the light of this article — was also reported in [8] where the Q-factor of a reverberation chamber was found using the ray launching technique.

The main idea behind this method is to discretize the wavefront into a number of individual rays, each of which will carry a part of the total transmitted power. The net received power is therefore the superposition of all power components P_i (see Section 2) reaching the receiver.

The ray tracing method has two variations. One being the Image Method (IM) which basically consists in finding all images (virtual sources) of the real source with respect to all planes (walls) of the given environment. In the example arrangement of four walls in Figure 1(a), a propagation path with three reflections is found. To do so, I_3 image of the transmitter Tx is determined relative to plane 3. I_3 is next reflected relative to plane 4, thus producing image $I_{3,4}$. Finally, $I_{3,4,2}$ is obtained by reflecting $I_{3,4}$ against plane 2. Once the procedure is finished, a receiver Rx is located at a desired place and the propagation path with three reflections is determined by tracing back through the intersection points $r_1 \rightarrow r_2 \rightarrow r_3$. Similarly, propagation paths can be found for any number of reflections. A great advantage of this method is that for a given location of transmitter, the path tracing procedure need be carried out only once, irrespective of the later receiver locations.

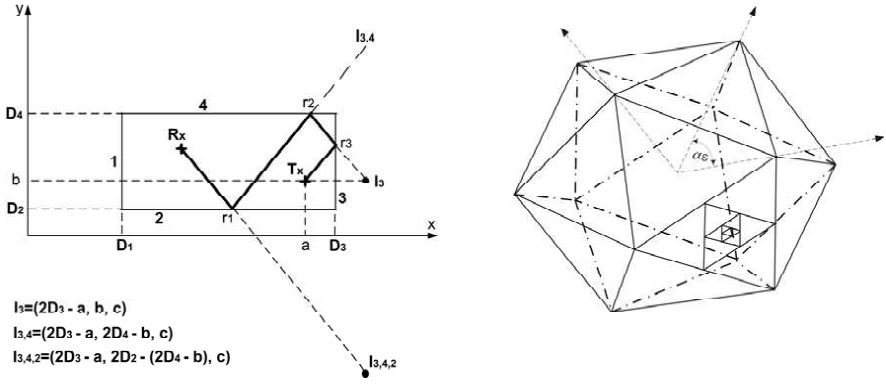

(a) (b)

Figure 1. A principle of (a) the image method (b) and the ray launching.

In the Ray Launching (RL) method, transmitted wave is discretized into N rays with equal angular separations α_s. By doing so, each ray will carry a portion of power proportional to the solid angle between any neighboring rays. In order to assure a constant α_s, the radiation sphere is first approximated with an icosahedron with 12 vertices and $\alpha_s = 65.5^\circ$ between neighboring vertices (see Figure 1(b)). Since such a low resolution is unacceptable, new vertices are generated by tessellating each of the 20 triangles of the solid. This is done by joining the midpoints of every triplet of neighboring sides into smaller triangles thus obtaining a greater number of vertices (and, consequently, smaller angular separation) than from the original icosahedron (as proposed in [9]).

If the rays resolution is still unsatisfactory, the tessellation process can be repeated T times, where T is the *tessellation frequency* and is incremented by one after each tessellation (starting with $T = 1$ for the initial, untessellated icosahedron). The total number of rays $N(T)$ that can be launched is therefore equal to the number of vertices after T tessellations and is given by (1). The RL method also lends itself for modeling arbitrary Antenna Radiation Pattern (ARP), in which case however, one must take care to assure a proper value of $N(T)$ since rays — if launched too sparsely — may omit some crucial features of the modeled ARP. It was demonstrated in [10] that for all several investigated antennas, the sufficient density of rays to almost ideally represent the respective ARP, was obtained for $T = 6$ (which corresponds to the total of 10242 rays). As a measure of accuracy the calculated power gain vs. the measured gain for those antennas, was taken. This result can be considered as a reasonable trade-off between the time of execution of the RL procedure (linearly proportional to the number of rays) and the accuracy in reproducing the original ARP.

$$N(T) = 10 \cdot 4^{T-1} + 2 \tag{1}$$

For the sake of completeness, it should be added that in the course of research performed in [10] it was also determined that for typical indoors (such as offices, cubicles, halls etc.) the value of at least $T = 7$, or $N(T = 7) = 40962$, is necessary to assure that even the smallest modeled geometrical features will not be omitted by rays diverging from the source. This result was maintained for the rest of the investigations presented in this paper as well.

In the paper, some observations are provided regarding the use of the RL method to simulate the radio channel in the reverberation chamber. All presented investigations will be split into two domains: the electromagnetic (EM) power P_{EM} distribution and the time characteristic represented by the time delay spread τ_{RMS} and discussed shortly in Section 2.

2. THEORY BEHIND THE TIME DELAY SPREAD

The analysis of the radio channels as a time-dispersive medium shall start with the observation that the emitted signal will propagate by interacting with the surrounding environment, that involves reflections from objects, transmissions thru obstacles, diffraction on edges and scattering from rough surface. Thus, the signal arriving at the receiver will not come in a single fringe, but as a pack of signals with different amplitudes, phases, angles of arrival, and short time delays, being delayed copies of the original signal (refer to [11] for more details). A numeric measure of describing this multipath effect is termed as the time delay spread, τ_{rms}, defined by (2) for discrete radio channels. It accounts for all power echoes $P_i(\tau_i)$ arrived at the receiver with a delay of τ_i, while τ_m denotes the mean delay 3). Each i-th power component corresponds to one of the $N(T)$ launched rays, as described in Section 1. It is worth to note that τ_{rms} is the second central moment of a squared channel impulse response (called the Power Delay Profile, PDP).

$$\tau_{rms} = \sqrt{\frac{\sum\limits_{i} (\tau_i - \tau_m)^2 P(\tau_i)}{\sum\limits_{i} P(\tau_i)}} \tag{2}$$

$$\tau_m = \frac{\sum\limits_{i} \tau_i P(\tau_i)}{\sum\limits_{i} P(\tau_i)} \tag{3}$$

Describing the wireless channel with τ_{rms} is not a trivial task since the process of measuring (sounding) the channel PDP, from which τ_{rms} can then be estimated, usually requires a considerable amount of time. Moreover, it may happen that due to the time-variant nature of the wireless channel or upon appearance of interferences, the obtained results can be distorted. As the main sources of the described problems usually fall beyond researchers' control, a realistic wireless channel does not appear to be a good test environment mainly due to deficient reliability and controllability. For this reason some alternative solutions were extensively investigated. One alternative is to use the reverberation chamber (RC) (as in [11–15]) — a metallic shielded room with one or more stirrers (paddles) inside. It is noteworthy that the RC is in fact a resonant cavity of large dimensions, inside which the energy of the electromagnetic (EM) field is stored for the dwell-time duration which corresponds to τ_{rms}. The power distribution measured inside the test volume of the RC follows the exponential distribution since it is χ^2-distributed with two degrees of freedom whereas the

magnitude of any of the electric field components is χ-distributed and consequently has a Rayleigh distribution ([16, 17]). Such distributions further indicate that RCs can be considered as strongly multipath propagation environments. Therefore the RC lends itself for the use as a wireless channel emulator. However, in order to properly use the RC for this purpose, an in-depth know-how in this field is required, which can be reached by the two means: either by measurements or by numerical simulations. Due to the finite nature of the time budget usually assigned to complete the planned tasks, the approach based on measurements could appear to be a "never ending story". On the other hand simulations alone can not be treated as a reliable source of knowledge. Therefore the best of the worlds lies in the combination of measurements and simulations. The latter (i.e., simulations) though require that the RC is properly modeled, in terms of both its geometry and EM features such as the walls conductivity, and then tuned in order to yield representative results. This paper will focus on the aspect of tuning, with two main goals in the scope. The purpose of the first and the most important one (Sections 5 and 6) is to assign appropriate values to various parameters of the reverberation chamber model, such as the wall reflectivity loss, the receive probe size or the number o reflections — all in order to achieve convergence between outcomes obtained in the real chamber and those arrived at in the simulated one. This tuning process can be done in the time domain (convergence for τ_{rms}) or in the EM power domain (convergence for the electric field strength or the EM power distribution). The second, less crucial aspect, studied in this work (Section 3) consists in determination of optimal conditions under which simulations should be performed, which allows to accelerate simulations with no harm to the quality of achieved results. At this stage the minimum number of stirrer rotations (i.e., distinct angular positions) should be investigated, which is crucial for the EM field distribution (or its time properties) to assume appropriate statistical robustness and stability.

In the following sections, one will find more details regarding the tuning process of above-mentioned parameters.

3. THE ESTIMATION OF THE MINIMUM NUMBER OF STIRRER ROTATIONS

This section is devoted to the issue of the number of the stirrer rotations N_{ROT} considered in the simulations, which severely (and linearly) affects the total time of execution. The intention behind the investigations presented here is to estimate the minimum N_{ROT} which ensures satisfactory accuracy of predictions as compared to

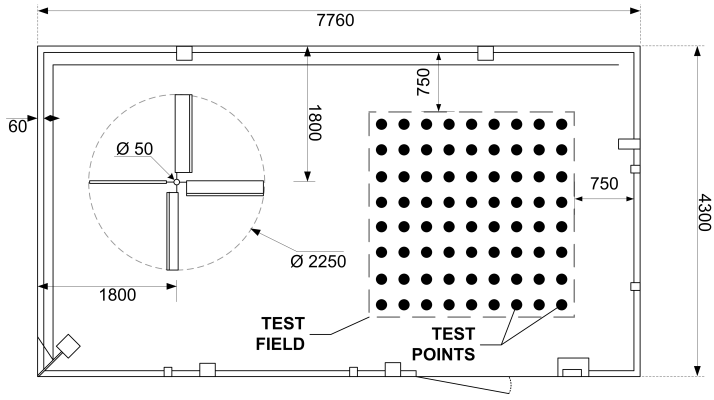

Figure 2. Top schematic view of the WrUT reverberation chamber.

the reference case with 72 rotations, at 5° steps at frequencies of 2.45 GHz and 5.75 GHz. The reference values for both τ_{RMS} and EM power (P_{EM}) were found by means of averaging the time delay spread (or EM power readings) obtained in 72 locations — test points in Figure 2 inside the reverberation chamber, averaged over 72 rotations (accidental coincidence of numbers).

Firstly, the average τ_{RMS} (or EM power) in those locations was determined for a single ($N_{ROT} = 1$) randomly chosen stirrer position out of 72 available ones. This procedure was then repeated 100 times for $N_{ROT} = 1$ random positions yielding a set of 100 vertically aligned points visible in Figure 3. Thereupon, N_{ROT} was incremented by a unity ($N_{ROT} = 2$) and the routine was repeated for a hundred random stirrer position pairs producing another set of vertical points and so forth until and including $N_{ROT} = 71$.

The observed values of the delay spread have an easy to perceive down-tilted trend (bold line) with the regression line parameters (τ_{RMS_reg}) provided in Figure 3(a). It can also be observed that the delay spread values tend to scatter less about the trend line as N_{ROT} grows (see the dashed line representing the standard deviation of simulated samples). In the worst case with just a single stirrer position ($N_{ROT} = 1$), the maximum mismatch between the final value of $\tau_{RMS} = 1135.2$ ns (at $N_{ROT} = 72$) and the simulated value equals 14.3 ns. As for the EM power (Figure 3(b)), the simulated values attained for a single stirrer rotation ($N_{ROT} = 1$) are scattered by a maximum of 0.16 dB relative to the final value (which was 8.54 dBm at $N_{ROT} = 72$). These results, for both the time delay spread and the EM power, can be interpreted as a degree of expected error created when

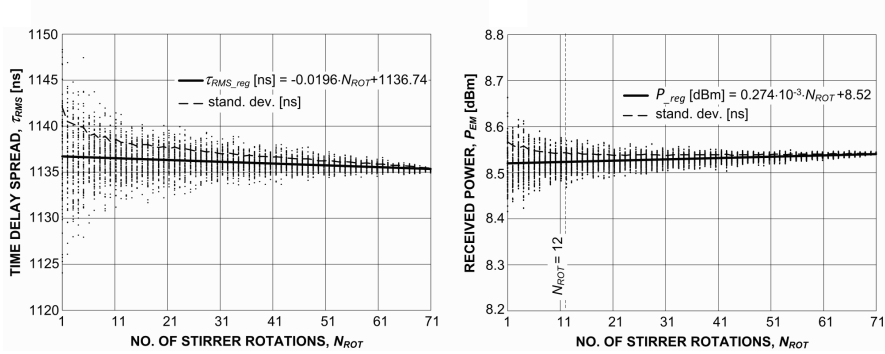

(a) (b)

Figure 3. Convergence of the simulated (a) τ_{RMS} and (b) P_{EM} with increasing number of stirrer rotations N_{ROT}.

simulations constrained to a single stirrer rotation are to be considered as representative to those averaged over all rotations. Consequently, such a simplification of procedure will yield an expected error of 1.26% and 1.87% for τ_{RMS} and P_{EM}, respectively.

Probably for most situations such errors would be quite acceptable, however to be consistent with practices recommended regarding the necessary number of stirrer rotations in real measurements for reverberation chambers, one may choose to perform simulations at 12 random rotations (as advised in [18] for the electric field strength measurements at frequencies discussed in the paper, i.e., 10 times the RC lowest usable frequency). With this N_{ROT}, simulations will render the expected error of 0.6% and 0.7% for τ_{RMS} and P_{EM}, respectively.

4. INFLUENCE OF THE NUMBER OF REFLECTIONS

The ray launching is inherently associated with the notion of the number of reflections N_{REF} to be considered in the procedure. Each i-th traced ray carries a portion of the output transmitter power — $P_{EM}^{out}/N(T)$, resulting form its direction (due to its ARP being a two-parameter function of direction in the horizontal θ and vertical ϕ plane), then augmented by the directional transmit antenna gain $G_{Tx}(\theta,\phi)$ and diminished by the pathloss L. This output energy of a single i-th ray ($P_{EM}^{out|dB}$) is therefore given by (4). In regular, highly attenuating environments with partitions (walls, ceilings, persons etc.), the power of a statistical ray will drop below a significant level after several reflections from obstacles or transmissions thru

them. In reverberation chambers, however, the signal propagation is predominated by reflections in the absence of dividing partitions, usually also with few absorbing objects (such as devices under test, intentionally placed absorbers for controlling the time delay spread or supports and mountings made of plastic or wood). Under such circumstances it should be assumed that the number of reflections from walls and the stirrer may be remarkable, especially if one recalls that expected reflection losses from metallic surfaces are on the order of a hundredth of a decibel. A particular care must be taken of selecting a proper value of a singular reflection loss Γ, keeping in mind that it is next going to be used N_{REF} times for each ray. A reasonable solution would be to calculate this loss from the conductivity characteristic to the metal composing the walls, however such material data is usually not specified by the chamber manufacturers, except general statements in the documentation indicating only the kind of metal used for production — most often aluminium or its alloy. It can be therefore recommended to adjust Γ by exactly modeling the chamber configuration and then performing both simulations and measurements (of the received electromagnetic power or the time delay spread), preferably with all absorbing objects removed for better control of the reverberating properties of the chamber. This removal is to minimize any additional contributions of energy scattering/absorption, other than metallic walls or the paddle, of which cumulative effect would otherwise add extra losses — another potential source of mismatch between simulations and measurements.

$$P_{EM}^{i,Tx}(\theta,\phi)_{|dB} = P_{EM}^{out|dB} + G_{Tx|dB}(\theta,\phi) - 10\log N(T) \tag{4}$$

While traversing the chamber, the ray experiences multiple losses from numerous reflections. Thus, upon reception the i-th ray power will have decreased to a level determined by the N_{REF} multiples of a singular reflection loss Γ (beside additional losses L due to the presence of absorbing materials) and amplified by the receive antenna directional gain $G_{Rx}(\theta,\phi)$, as in (5).

$$P_{EM}^{i,Rx}(\theta,\phi)_{|dB} = P_{EM}^{i,Tx}(\theta,\phi)_{|dB} + G_{Rx|dB}(\theta,\phi) - N_{REF}\cdot\Gamma_{|dB} - L_{|dB} \tag{5}$$

For the purpose of assessing the effect of the chosen number of simulations on the simulated EM power and the time delay spread, a number of simulations have been carried out in which N_{REF} was varied from 1 to 2600 for frequencies 2.45 GHz and 5.75 GHz (to which the model presented in [11] was tuned). The results, being the average of samples collected in 72 points (see Figure 2) in the chamber, are discussed separately for the simulated τ_{RMS} (Figure 4) and P_{EM} (Figure 5). These have been calculated for 44 discrete values of N_{REF}, i.e., $1, 2, \ldots, 10, 20, \ldots, 100, 200, \ldots, 2600$ taking the singular reflection

loss Γ or the probe size D as variable parameters for τ_{RMS} and P_{EM}, respectively. The reason why different parameters are considered for the EM power and the time domain investigations will be explained in more detail in Section 5. For now, it should suffice to know that the time delay spread and EM power respond oppositely to changes in the reflection loss and the probe diameter, namely — τ_{RMS} reacts dynamically to changes in Γ but remains unaffected by D whereas P_{EM} exhibits quite inverse behavior.

The first-glance observation (Figure 4) shows that for a decreasing Γ a greater number of reflections is necessary to achieve the flat region of τ_{RMS}. From this behavior, one can conclude that the correct value of Γ should found by adjusting its value until the simulated time delay spread (obtained with a given Γ) is comparable to that measured in an unloaded chamber. For all further simulations this value will hold unchanged for the frequency at which the tuning was made.

For example, during the tuning process described in [11] an optimal singular reflection loss Γ of $8.0 \cdot 10^{-3}$ dB was found at 2.45 GHz from comparative analyses between the measured ($\tau_{RMS} = 1.6\,\mu$s) and the simulated ($\tau_{RMS} = 1.61\,\mu$s) values in the reverberation chamber located at Wroclaw University of Technology (WrUT). Similar conclusions can be applied to the EM power which tends to grow as the probe size D is being increased (Figure 5), but flattens out at a much faster rate with N_{REF} than τ_{RMS}. The outcomes straightforwardly indicate that as for τ_{RMS} the simulated values converge to stability at N_{REF} far greater (on the order of ten times) than that for EM power. For the cited value of $\Gamma = 0.008$ dB the necessary N_{REF} turns out to be equal 2500, whereas the EM power converges to a stable value at N_{REF} close to 100 at $D = 0.03$ cm, both Γ and D optimized for WrUT reverberation chamber.

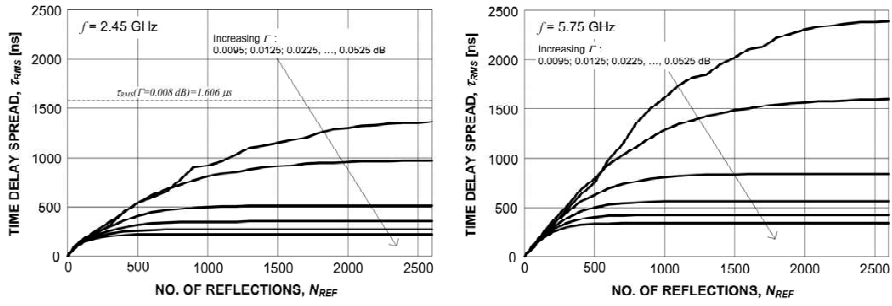

(a) (b)

Figure 4. Simulated values of the time delay spread at (a) 2.45 GHz; (b) 5.75 GHz vs. the number of reflections.

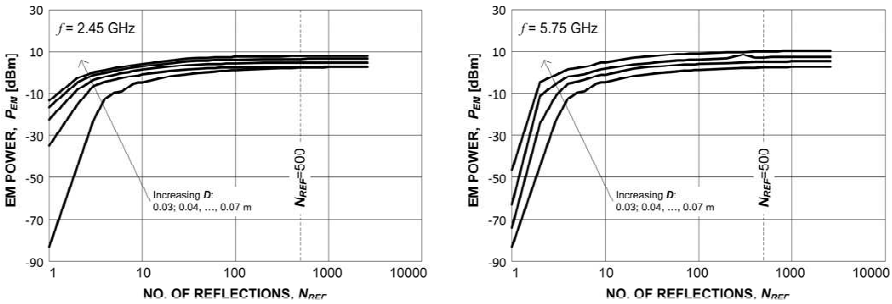

Figure 5. Simulated values of the EM power at (a) 2.45 GHz; (b) 5.75 GHz vs. the number of reflections.

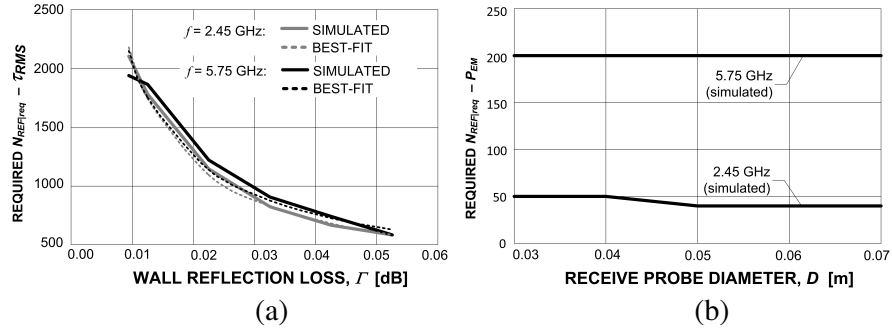

Figure 6. Minimum required number of reflections in (a) the time delay spread and (b) the EM power simulations.

These observations are more conveniently visualized when the outcomes are plotted as a minimum necessary number of reflections vs. Γ and D for each discrete value of the latter parameters, as shown in Figure 6. The "minimum" N_{REF} in this case is understood as such for which the ratio $\tau_{RMS}(k)/\tau_{RMS}(k-1)$ or $P_{EM}(k)/P_{EM}(k-1)$ is less than 1%, where k is the position in the set of 44 discrete values of N_{REF} mentioned above (for instance the value τ_{RMS} obtained at $N_{REF} = 200$ divided by τ_{RMS} obtained at $N_{REF} = 100$). It corresponds to the point on a given curve in Figure 4 and Figure 5 from which it is further considered flat.

It can be seen in Figure 6(a) that for the time delay spread, $N_{REF|req}$ required to achieve the stable region (as plotted in Figure 4) varies with Γ exponentially as in Equation (6). On the other hand, the

EM power is almost constant for most values of D and equals 200 at 5.75 GHz and 40–50 at 2.45 GHz (i.e., higher frequencies may require a higher-order N_{REF}).

$$N_{REF|req} = \begin{cases} 48.02 \cdot \Gamma^{-0.857} \text{ for 2.45 GHz} \\ 63.96 \cdot \Gamma^{-0.792} \text{ for 5.75 GHz} \end{cases} \quad (6)$$

It can be concluded from the above studies that since the parameter of interest can be either the EM power distribution or the signal time properties, different selection of N_{REF} must be made. N_{REF} is less restrictive for the power domain (stability is found at around 200 reflections), but more strict for the time domain investigations where at least a few hundred (up to c.a. 2500 for WrUT reverberation chamber) reflections should be taken into account to ensure that the obtained results will not vary considerably with later increases in N_{REF}. Moreover, due to linear dependence with N_{REF}, these settings will translate directly to the time length of the whole RL procedure execution. Lastly, it must be remembered that the plots in Figure 4 and Figure 5 may, and expectedly will, look different for reverberation chambers with different geometries than that in WrUT.

5. ON THE INFLUENCE OF THE WALLS REFLECTION LOSS AND THE RECEPTION PROBE SIZE

In this section, the influence has been analyzed of two parameters that need to be defined prior to simulations. These two are: the loss Γ incurred by the incident ray carrying power P_i upon reflection from the chamber wall (Figure 7(a)) and the simulated receive probe size (the diameter in Figure 7(b)).

It should be stressed, however, that despite the functional similarity, the receive probe in geometrical optics sense (which includes the RL) differs from the physical probes. It should be rather understood as a sphere (in the isotropic case) that collects multipath rays traversing the RC, hence the larger its size the more components will be captured, thus contributing to the increase in the total received EM power. The corresponding term "diameter" (or D used throughout the paper) in Figure 7(b) has therefore no relation to the physical size of the real probe but is a measure of the assumed reception sphere in the RL model (and which is subject to the tuning).

The issue which the authors attempt to answer is how these parameters influence both EM power and the time delay spread, as their values (i.e., D and Γ) are successively increased. It should be noted that (as also indicated in [19]) these parameters are the first candidates to modifications in the tuning procedure of the simulation

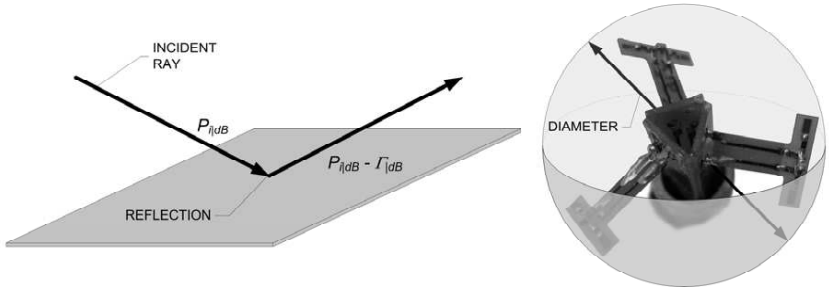

(a) (b)

Figure 7. Two simulation factor subject to tuning: (a) reflection loss Γ; (b) probe size (diameter).

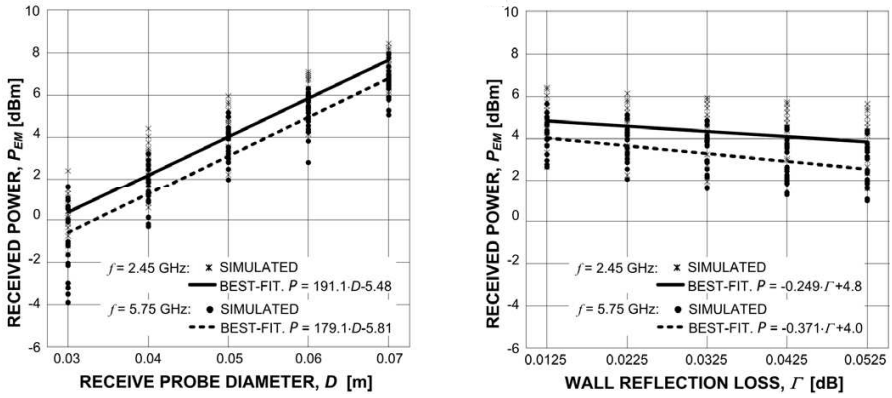

(a) (b)

Figure 8. Influence of (a) the probe size (diameter) D and (b) reflection loss Γ on the received power.

tool to the measured (reference) results (see multiple references to this subject in Section 4).

As can be observed in Figure 8 for the net received EM power P_{EM}, the value D assigned to the simulated probe strongly affects the readings. As the probe size was increased by four centimeters in total, the received power was increased by 7.8 dB and 7.3 dB for 2.45 GHz and 5.75 GHz, respectively. However, the total change in Γ by 0.04 dB resulted in merely 1 dB and 1.5 dB (for 2.45 GHz and 5.75 GHz, respectively). In the case of the time delay spread (Figure 9) the reaction to changes in D and Γ turned out to be

quite opposite. Namely, τ_{RMS} is apparently insensitive the probe size since it changed by only 24.6 ns and 7.5 ns (for 2.45 GHz and 5.75 GHz, respectively), compared to the average being on the order of a few hundred nanoseconds. The delay spread exhibited a strongly exponential profile with net changes equal to 905.7 ns and 1190.7 ns as the reflection losses changed from 0.0125 dB to 0.0525 dB, respectively. The effect is similar to that of laying absorbing panels on the chamber walls, reported in [11].

This section was considered to be of particular value to researchers attempting to tune their deterministic models to match the measured outcomes — i.e., the EM power distribution and the radio channel time characteristics inside the chamber. A practical remark that stems from the above observations is that in order to make the simulator produce reliable results (in both EM power and time domain) one needs to carefully adjust an optimal two-parameter operational point — the $< D; \Gamma >$ pair. However, it has just been demonstrated that changes in D affect severely only the received EM power which, in turn, appears to be negligibly dependent on Γ. On the other hand, the time delay spread responds dynamically only to changes in Γ but is basically unaffected by variations in D. Therefore, each of the two parameters (D, Γ) forming the best-matched pair, may be sought separately, which simplifies the tuning routine and reduces the problem from a two-parameter to a single-dimensional one.

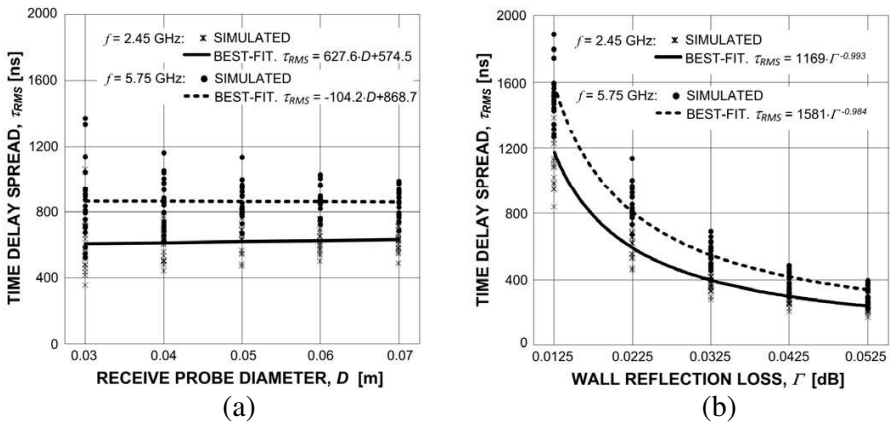

Figure 9. Influence of (a) the probe size (diameter) D and (b) reflection loss Γ on the time delay spread.

6. PRACTICAL REMARKS ON TUNING

Basing on investigations presented throughout the paper the authors have compiled the results into a set of simple steps, enumerated below, to facilitate the process of tuning the deterministic (RL-based) model to a particular reverberation chamber, utilizing some reference measurement outcomes. Firstly, the purpose will be to find the required number of reflections, secondly — an optimal value of Γ (for τ_{RMS}) or D (for EM power).

1. Perform reference measurements of the time delay spread (or the EM power) while the reverberation chamber is unloaded.
2. Create a geometrical model of the reverberation chamber and perform simulations of τ_{RMS} (or P_{EM}) for different values of Γ (or D) to produce a set of curves as in Figure 4 and Figure 5.
3. For τ_{RMS} determine the relationship $N_{REF|req}$ as a function of Γ, such as in Equation (6).
4. Find the required N_{REF} from the equation obtained during step No. 3 (for τ_{RMS}) or read the value directly from the obtained curve (for P_{EM}).
5. Choose a set of discrete values of Γ (or D) and perform simulations with N_{REF} determined during the step No. 4.

The value of Γ (or D) for which τ_{RMS} (or P_{EM}) best matches that obtained during reference measurements (step 1) can be considered optimal for all further simulations and the simulator can be regarded as properly tuned.

It should be added that while searching the optimal Γ for the time delay spread, D should be kept at reasonable value (resembling real physical dimensions of the receive probe). Similarly, in the process of finding the optimal D for the EM power investigations, Γ should be held constant at c.a. 0.001 dB.

7. CONCLUSIONS AND FURTHER RESEARCH

The paper can be treated as a discussion on the applicability of a deterministic model based on ray tracing (RT) for simulating the radio channel properties inside the reverberation chamber. Prior to analyses of the simulated outcomes, a brief introduction was made on general principles underlying two most popular versions of RT, i.e., the image method (IM) and the ray launching (RL). The latter method was given an in-depth attention throughout the rest of the article. Two parameters, namely the EM power (P_{EM}) and the time delay spread

(τ_{RMS}), were investigated with respect to their susceptibility to various RL settings. The first studies concerned the number of stirrer rotations necessary to obtain representative results, which concluded that both electric field parameters are rather well represented by even few stirrer positions (due to the chamber excellent reverberating properties that spread the electric field evenly quite irrespectively of internal elements positioning). As for the number of reflections — which was investigated next — it turned out that if simulations are used for obtaining EM power distribution, up to two hundred reflections of each ray are quite sufficient for stable results at 5.75 GHz while for 2.4 GHz even down to 40–50 reflections, unlike with the delay spread which required rays five times more reflections to stabilize. It should be noted that the time needed to perform the RL procedure in the simulator will be affected at the same rate, as being a linear function of the number of reflections. Lastly, some practical remarks were presented with regard to the selection of the receive probe size and the wall reflection loss — the two parameters which values affect the EM power and the delay spread, as was demonstrated, in quite an opposite manner. The most notable conclusion drawn from these investigations is that the optimal pair of these parameters can be obtained by separately adjusting each of them to the reference measurements. In the last chapter, the authors proposed a simple procedure for the tuning of the deterministic model based on the Ray Launching technique.

The authors are currently advanced in research on novel methods for controlling the time delay spread in the reverberation chamber, in order to recreate the desired multipath profile characteristic to any propagation environment.

ACKNOWLEDGMENT

This paper has been written as a result of realization of the project "Next generation services and teleinformatic networks — technical, application and market aspects — electromagnetic compatibility". The contract for refinancing No. PBZ-MNiSW 02/II/2007.

REFERENCES

1. El-Sallabi, H. M., G. Liang, H. L. Bertoni, I. T. Rekanos, and P. Vainikainen, "Influence of diffraction coefficient and corner shape on ray prediction of power and delay spread in urban microcells," *IEEE Transactions on Antennas and Propagation*, Vol. 50, No. 5, 703–712, May 2002.

2. Rodrigues, M. E. C., L. A. R. Ramirez, L. A. R. Silva Mello, and F. J. V. Hasselmann, "A ray tracing technique for coverage predictions in micro cellular environments," *Journal of Microwaves and Optoelectronics*, Vol. 3, No. 5, 1–17, Jul. 2004.
3. Rautiainen, T., G. Wölfle, and R. Hoppe, "Verifying path loss and delay spread predictions of a 3D ray tracing propagation model in urban environment," *IEEE 56th Vehicular Technology Conference*, Vol. 4, 2470–2474, Sep. 2002.
4. Rossi, J.-P. and Y. Gabillet, "A mixed ray launching/tracing method for full 3-D UHF propagation modeling and comparison with wide-band measurements," *IEEE Transactions on Antennas and Propagation*, Vol. 50, No. 4, 517–523, Apr. 2002.
5. Lee, B. S., A. R. Nix, and J. P. McGeehan, "Indoor space-time propagation modeling using a ray launching technique," *IEE, 71st International Conference on Antennas and Propagation*, No. 480, 279–283, Apr. 17–20, 2001.
6. Wang, Y., S. Safavi-Naeini, and S. K. Haudhuri, "A hybrid technique based on combining ray tracing and FDTD methods for site-specific modelling of indoor radio wave propagation," *IEEE Transactions on Antennas and Propagation*, Vol. 48, No. 5, 743–754, May 2000.
7. Ji, Z., B.-H. Li, H.-X. Wang, H.-Y. Chen, and T. K. Sarkar, "Efficient ray-tracing methods for propagation prediction for indoor wireless communications," *IEEE Antennas and Propagation Magazine*, Vol. 43, No. 2, 41–49, Apr. 2001.
8. Kwon, D.-H., R. J. Burkholder, and P. H. Pathak, "Ray analysis of electromagnetic field build-up and quality factor of electrically large shielded enclosures," *IEEE Transactions on Electromagnetic Compatibility*, Vol. 40, No. 1, 19–26, Feb. 1998.
9. Tan, S. Y. and H. S. Tan, "Modelling and measurements of channel impulse response for an indoor wireless communication system," *Proc. IEE Microwaves, Antennas and Propagation*, Vol. 142, No. 5, 405–410, Oct. 1995.
10. Staniec, K., "The indoor radiowave propagation modeling in ISM bands for broadband wireless systems," Ph.D. Dissertation, Wroclaw University of Technology, Poland, 2006.
11. Pomianek, A. J., K. Staniec, and Z. Joskiewicz, "Practical remarks on measurement and simulation methods to emulate the wireless channel in the reverberation chamber," *Progress In Electromagnetic Research*, Vol. 105, 49–69, 2010.
12. Genender, E., C. L. Holloway, K. A. Remley, J. Ladbury, G. Koepke, and H. Garbe, "Use of reverberation chamber to

simulate the power delay profile of a wireless environment," *Proc. International Symposium on Electromagnetic Compatibility — EMC Europe*, 1–6, Hamburg, Sep. 8–12, 2008.

13. Orlenius, C., M. Franzen, P. S. Kildal, and U. Carlberg, "Investigation of heavily loaded reverberation chamber for testing of wideband wireless units," *IEEE International Symposium on Antenna Propagation*, 3567–3572, Jul. 2006.
14. Hallbjorner, P., M. Grudén, and M. Jobs, "Broadband space-time measurements in reverberation chamber including comparison with real time environment," *IEEE Antennas and Wireless Propagation Letters*, Vol. 8, 1111–1114, 2009.
15. Corona, P., G. Ferrara, and M. Migliaccio, "Reverberating chambers as sources of stochastic electromagnetic fields," *IEEE Transactions on Electromagnetic Compatibility*, Vol. 38, No. 3, 348–356, Aug. 1996.
16. Hill, D. A., *Electromagnetic Fields in Cavities: Deterministic and Statistical Theories*, Wiley-IEEE Press, Oct. 2009.
17. Yu, S.-P. and C. F. Bunting, "Statistical investigation of frequency-stirred reverberation chambers," *Proc. 2003 IEEE International Symposium on Electromagnetic Compatibility*, Vol. 1, 155–159, Istanbul, Turkey, Aug. 18–22, 2003.
18. IEC 61000-4-21 Electromagnetic compatibility (EMC) Part 4: Testing and measurement techniques Reverberation chamber test methods. Section 21: Reverberation Chamber Test Methods.
19. Staniec, K., "Notes on the tuning of a deterministic propagation model in the reverberation chamber," *Proc. 2010 Asia-Pacific Symposium on Electromagnetic Compatibility APEMC*, 893–896, Beijing, China, Apr. 12–16, 2010.